General Disclaimer

One or more of the Following Statements may affect this Document

- This document has been reproduced from the best copy furnished by the organizational source. It is being released in the interest of making available as much information as possible.

- This document may contain data, which exceeds the sheet parameters. It was furnished in this condition by the organizational source and is the best copy available.

- This document may contain tone-on-tone or color graphs, charts and/or pictures, which have been reproduced in black and white.

- This document is paginated as submitted by the original source.

- Portions of this document are not fully legible due to the historical nature of some of the material. However, it is the best reproduction available from the original submission.

13

COO-1764-112

A Facsimile Report

Reproduced by
UNITED STATES
ATOMIC ENERGY COMMISSION
Division of Technical Information
P.O. Box 62 Oak Ridge, Tennessee 37830

Sgt-64929R

Measurements of π^-p Elastic Scattering from 1.71 to 5.53 GeV/c*

M. Fellinger, E. Gutman, R. C. Lamb, F. C. Peterson, and L. S. Schroeder

Institute for Atomic Research and Department of Physics

Iowa State University, Ames, Iowa 50010

and

R. C. Chase,† E. Coleman, and T. G. Rhoades‡

School of Physics, University of Minnesota, Minneapolis, Minnesota 55455

ABSTRACT

The π^-p elastic scattering differential cross section has been obtained at eighteen incident momenta from 1.71 to 5.53 GeV/c. The measurements were taken over a limited range of squared four-momentum transfer, t, near the forward direction. The statistical accuracy and resolution of these data are comparable to, or better than, existing data. The parameter b in the expression $d\sigma/dt = Ae^{bt}$ has been determined at each of our incident momenta, and a large (~25%) enhancement in b as a function of momentum is observed at a center of mass energy of ~2290 MeV. The relation of this bump in b with the well established bump in the total π^-p cross section at ~2200 MeV is discussed.

---

*Work was supported in part by the Ames Laboratory of the U. S. Atomic Energy Commission (Contribution No. 2762) and the National Aeronautics and Space Administration.

†Present address: American Science Engineering, Cambridge, Mass. 02142.

‡Present address: Department of Physics, University of Birmingham, Edg Baston, Birmingham 15, England.

I. INTRODUCTION

In a recent experiment at the Argonne National Laboratory Zero-Gradient-Synchrotron (ZGS), we measured the differential cross section for the elastic scattering of negative pions from deuterium at 2.01, 3.77, and 5.53 GeV/c.[1] To check the acceptance of our apparatus we made measurements of the process $\pi^-p \to \pi^-p$ over a similar momentum range and compared them with existing π^-p elastic scattering measurements.[2-4] In this paper we present the π^-p measurements. The measurements were made at twelve incident pion momenta in the range from 1.71 to 2.76 GeV/c and also at 3.01, 3.52, 3.77, 4.02, 5.03, and 5.53 GeV/c. The closely spaced 1.71 to 2.76 GeV/c data were taken to help settle the question of what nucleon resonances are present in the mass region of the N(2190).

Our data are in agreement with previous measurements,[2-4] and in the 1.71 to 2.76 GeV/c region have somewhat superior statistical accuracy than previous results. These data coupled with polarization measurements of the same process[4] have proved useful in providing additional evidence for a nucleon resonance in the H_{19} partial wave at a mass value of 2245 MeV.[5] Our data are confined to a limited angular region; in terms of t, the squared four-momentum transfer, the data cover a t interval of approximately -0.2 to -0.7 $(GeV/c)^2$.

Section II gives the details of our experimental method. Section III presents the differential cross sections in tabular form, as well as the momentum variation of the parameter b in the expression $d\sigma/dt = Ae^{bt}$. This exponential slope, b, shows about a 25% increase at center of mass energy of 2190 MeV, significantly higher in mass than the well known bump in the π^-p total cross section near 2200 MeV.[6,7]

II. EXPERIMENTAL METHOD

The experiment was performed in the 17° beam of the ZGS. The beam transport system determined the momentum of the pions to ±1% and brought the beam to a final focus on a 2.31 in.-long liquid-hydrogen target. The beam intensity varied from (1 to 7) x 10^5 pions/pulse depending on the beam momentum, with a pulse repetition rate of 1000 pulses/h. The beam angular divergence was ±5 mrad horizontally and ±3 mrad vertically. The experimental apparatus used to detect the elastic events is shown in Fig. 1. The pion beam was detected by a series of scintillation counters labeled S_1, S_2, S_3, and S_4. Counters S_1 and S_2 are not shown in the figure and are located near the first focus of the 17° beam. The beam size was defined by S_4, a $\frac{3}{4}$-in. x $\frac{3}{4}$-in. counter.

Elastic events were detected in a double-arm spectrometer consisting of the two bending magnets M1 and M2 and scintillation counter arrays A, B, and P. Each of the A and B arrays consisted of 16 elements; the P array consisted of 30 elements. The dimensions for the A, B, and P elements are shown on Fig. 1. Negative particles traversed M1 and were detected by pairs of corresponding A and B elements. The width of an A array element determined the scattering-angle acceptance for each data point. The 16 pairs of corresponding A and B counters allowed 16 simultaneous differential cross sections to be measured. A single scintillation counter G behind the A-array determined the azimuthal angular acceptance. The recoil protons traversed M2 and were detected by the P array. The V1 and V2 counters were used to veto particles which did not satisfy the angular restrictions of πp elastic-scattering kinematics. The V3 counter was used as an additional

anticoincidence counter to veto beam pions that did not interact in the target. Events satisfying the following electronic coincidence requirements were selected and stored in a multichannel analyzer: (a) a count in beam counters ($S_1S_2S_3S_4$), (b) no count in veto counters ($\bar{V}_1\bar{V}_2\bar{V}_3$), (c) a count in corresponding A and B counters in coincidence with a count in <u>any</u> of the P counters, and (d) a count in G. These events were sorted into 16 different groups corresponding to the 16 AB pairs. For each pair the distribution of events along the P array was obtained.

Figure 2 shows some typical data accumulated for a beam momentum of 2.01 GeV/c. There are 16 separate distributions labelled 1 through 16 corresponding to increasing pion scattering angle. In each of the distributions the elastic-scattering events appear as a peak with a background of less than 1%. Since the acceptance of our apparatus varies slowly with angle, one can roughly see in Fig. 2 the variation in the differential cross section as a function of pion scattering angle. Also one can see the variation in the recoil proton direction. The data were displayed in this manner simultaneously with the running of the experiment so that any trouble that developed would have been readily detected. It took 6 hours to accumulate the data shown in Fig. 2. These particular data are all of the data at 2.01 GeV/c. The positions of the elastic peaks agree with predictions of a Monte Carlo simulation of the experiment.

III. RESULTS

The differential cross section is given by the formula

$$d\sigma/dt = F/N_\pi N_p \Delta t \ ,$$

where E is the number of events, N_π is the number of incident pions, N_p is the number/cm^2 of target protons, and Δt is the interval of the squared four-momentum transfer associated with the instrumental solid angle. The number of events was determined from the counts in the elastic peak, the number of beam pions was determined from the number of beam counts, $S_1S_2S_3S_4$, and the number of protons/cm^2 was determined from a knowledge of the length of the target and the known density of liquid hydrogen at an operating pressure of 1 atm. The solid angle was determined by a straightforward hand calculation and checked independently by a Monte Carlo computer program.

Corrections were applied to the data for muon and electron contamination of the pion beam, for decay of the scattered pion, for electronic deadtime effects due to V1, V2, and V3, and for absorption of particles in scintillators, liquid hydrogen, and other material. The combined correction due to these effects was typically 20%.

Table I lists the eighteen momenta at which the experiment was performed, the t-range covered[8] at each momentum, and the statistical accuracy of the differential cross sections. The elastic differential cross sections for the eighteen momenta are tabulated in Table II along with their associated errors. The quoted errors are statistical errors associated with event counts only. The relative normalization error between any two of our data sets at different momenta is less than 2%. In addition there is an over-all absolute uncertainty of ±5% to be uniformly associated with all data points.

The present data have been compared with other measurements[2-4] at the same or nearby momenta and are in good agreement. The extent of this

agreement as well as the quality of our data is illustrated in Fig. 3, where we have plotted our data at two momenta and data from other experiments at similar momenta.

In an effort to arrive at a simplified understanding of these cross section measurements we have fit the differential cross sections at each momentum to an expression of the form

$$d\sigma/dt = A e^{bt} ,$$

a form suggested by a small angle approximation to an optical model of high energy scattering[9] and employed extensively to parametrize small angle scattering data. A least-squares fitting procedure determined the coefficients A and b at each of the 18 momenta. In order to arrive at reasonable chi-squares, it was necessary to restrict the fit to data points for which $|t| \leq 0.63$ (GeV/c)^2. Beyond this value of t the differential cross section has a secondary peak or "shoulder" and deviates drastically from a simple exponential dependence on t. The values of b obtained from this procedure are listed in Table III and plotted in the lower half of Fig. 4. In the upper half of Fig. 4, we have plotted the π^-p total cross section taken from Carter et al.[7] and Citron et al.[10] Note the large bump in b (approximately 25%) in the vicinity of the ~8% bump in the total cross section, usually attributed to the N(2190) $J^P = 7/2^-$. The central position of the bump in b is at a value of $P_{LAB} \approx 2.3$ GeV/c while the position of the bump in σ_T is at a value of $P_{LAB} \approx 2.1$ GeV/c. The corresponding center of mass energies at these momenta are ≈ 2290 MeV and ≈ 2200 MeV, respectively. We would like to make the following two points: First, the bump in b

is due to the presence of direct channel resonances. The evidence for the correlation of variations in b with direct channel resonances has been extensively presented by Lasinski, Levi Setti, and Predazzi.[11] Second, the shift in the position of the bump from ~2200 MeV in σ_T to ~2290 in b can be understood in terms of the simple phenomenological model used in Ref. 11. In this model the scattering amplitude at small angles has two contributions, one due to diffraction scattering and the second due to direct channel resonance formation. As a consequence of this model Lasinski et al. demonstrate that resonances of different spin contribute to structure in b with a relative weight which is different than the relative weight with which they contribute to structure in σ_T. For a given resonance elasticity the weighting factor increases with increasing spin more rapidly for b than for σ_T. Therefore, one qualitative explanation for the mass difference in the positions of the bumps is that there are several resonances of different spin in this mass region, and the higher spin resonances have greater mass. A similar, but more precise, conclusion is reached by the authors of Ref. 5. Their detailed examination of our data and polarization data[4] provides evidence for two nucleon resonances in this energy region: one at 2245 MeV in the H_{19} partial wave, and one at 2260 MeV in the G_{17} partial wave. This latter resonance is the familiar N(2190). As the authors of Ref. 5 demonstrate, the bump in the total cross section at a mass value of 2200 MeV is due to these two high spin resonances plus the $D_{13}(2040)$ resonance.

ACKNOWLEDGMENTS

We appreciate the fine technical support offered by the Zero-Gradient Synchrotron personnel, in particular Tony Passi. We thank Dr. R. A. Lundy for a very helpful experimental suggestion, Professor A. D. Krisch for suggesting the measurements in the region of the N(2190), and Professor R. A. Leacock for useful discussions. We appreciate the assistance of P. N. Scharbach, G. Mrozek, and T. Curtright during part of the experiment. We also appreciate the capable technical help of Stephen Mosher and William Glass of Ames Laboratory.

REFERENCES

1. M. Fellinger, E. Gutman, R. C. Lamb, F. C. Peterson, L. S. Schroeder, R. C. Chase, E. Coleman, and T. G. Rhoades, Phys. Rev. Letters 22, 1265 (1969).
2. C. T. Coffin, N. Dikmen, L. Ettlinger, D. Meyer, A. Saulys, K. Terwilliger, and D. Williams, Phys. Rev. 159, 1169 (1967).
3. W. Busza, B. G. Duff, D. A. Garbutt, F. F. Heymann, C. C. Nimmon, K. M. Potter, T. P. Swetman, E. H. Bellamy, T. F. Buckley, R. W. Dobinson, P. V. March, J. A. Strong, and R. N. F. Walker, Phys. Rev. 180, 1339 (1969).
4. References to other $\pi^- p$ elastic scattering data may be found in A Compilation of Pion-Nucleon Scattering Data by G. Giacomelli, P. Pini, and S. Stazni, CERN/HERA 69-1 (unpublished) available in the U.S.A. from the Lawrence Radiation Laboratory, Berkeley, and in Europe from CERN, Geneva.
5. J. R. Hull and R. A. Leacock, see following paper.
6. A. N. Diddens, E. W. Jenkins, T. F. Kycia, and K. F. Riley, Phys. Rev. Letters 10, 262 (1963).
7. A. A. Carter, K. F. Riley, R. J. Tapper, D. V. Bugg, R. S. Gilmore, K. M. Knight, D. C. Salter, G. H. Stafford, E. J. N. Wilson, J. D. Davies, J. D. Dowell, P. M. Hattersley, R. I. Homer, and A. W. O'Dell, Phys. Rev. 168, 1457 (1968).

8. The measurements from 1.71 to 2.76 GeV/c were made with the bending magnet M1 at a fixed angle of 25° with respect to the incident beam line. The magnet current was set to bend a particle with the beam momentum through 10° at each momentum. Consequently, with the fixed bend angle and approximately fixed counter positions at each run, the t-range covered at each momentum moved to larger values of t as the beam momentum increased, as indicated in Table I.
9. See for example lectures by A. M. Wetherell on High Energy Scattering CERN 65-24 (unpublished); and M. L. Perl, L. W. Jones, and C. C. Ting, Phys. Rev. 132, 1252 (1963).
10. A. Citron, W. Galbraith, T. F. Kycia, B. A. Leontic, R. H. Phillips, A. Rousset, and P. H. Sharp, Phys. Rev. 144, 1101 (1966).
11. T. Lasinski, R. Levi Setti, and E. Predazzi, Phys. Rev. 179, 1426 (1969).

Table I. Summary of experiment.

Incident momentum (GeV/c)	$\|t\|$ range covered $(GeV/c)^2$	Statistical accuracy of data (%)
1.71	0.17-0.37	5.0-6.0
1.81	0.19-0.41	3.0-5.5
1.91	0.24-0.45	3.5-7.0
2.01	0.24-0.49	3.5-8.0
2.09	0.26-0.53	3.5-8.5
2.16	0.27-0.56	2.0-7.0
2.23	0.29-0.60	3.5-15.0
2.31	0.31-0.64	3.5-11.5
2.41	0.34-0.69	3.5-12.5
2.51	0.36-0.74	4.0-13.0
2.62	0.39-0.80	3.0-10.0
2.76	0.43-0.88	5.0-14.0
3.01	0.51-0.88	6.0-10.0
3.52	0.29-0.57	4.5-12.0
3.77	0.24-0.56	4.0-13.0
4.02	0.27-0.55	4.0-9.5
5.03	0.27-0.63	3.5-10.0
5.53	0.28-0.62	3.5-9.5

Table II. $\pi^- p$ elastic scattering.

$-t$ $(GeV/c)^2$	$d\sigma/dt$ $mb/(GeV/c)^2$	Statistical error $mb/(GeV/c)^2$	$-t$ $(GeV/c)^2$	$d\sigma/dt$ $mb/(GeV/c)^2$	Statistical error $mb/(GeV/c)^2$
	1.71 GeV/c		0.289	7.62	0.28
0.177	17.87	0.99	0.303	6.26	0.25
0.188	16.10	0.91	0.317	6.05	0.24
0.199	14.61	0.85	0.332	5.06	0.22
0.211	14.15	0.82	0.346	4.78	0.21
0.235	11.88	0.73	0.361	4.14	0.20
0.259	9.36	0.34	0.376	3.73	0.19
0.285	7.29	0.29	0.392	3.54	0.18
0.299	6.63	0.28	0.407	3.09	0.17
0.312	5.95	0.26			
0.325	5.64	0.26		1.91 GeV/c	
0.339	4.98	0.24	0.247	10.12	0.35
0.367	4.16	0.23	0.260	9.00	0.32
			0.275	7.60	0.29
	1.81 GeV/c		0.290	7.01	0.28
0.197	13.61	0.42	0.304	6.18	0.25
0.210	12.78	0.40	0.320	5.51	0.24
0.222	12.47	0.39	0.335	4.68	0.21
0.235	11.03	0.36	0.351	4.36	0.20
0.248	9.52	0.33	0.367	4.00	0.19
0.262	8.35	0.30	0.383	3.49	0.18
0.275	7.52	0.28	0.400	3.16	0.17

MORE

Table II. (continued)

$-t$ $(GeV/c)^2$	$d\sigma/dt$ $mb/(GeV/c)^2$	Statistical error $mb/(GeV/c)^2$
0.416	2.75	0.16
0.433	2.17	0.15
0.450	1.99	0.14
	2.01 GeV/c	
0.241	9.19	0.31
0.256	8.49	0.29
0.271	7.97	0.27
0.287	6.33	0.24
0.303	5.99	0.23
0.318	5.18	0.21
0.335	4.25	0.18
0.352	3.79	0.17
0.369	2.99	0.15
0.386	3.03	0.15
0.404	2.56	0.13
0.421	2.01	0.12
0.439	1.94	0.12
0.457	1.87	0.12
0.475	1.60	0.11
0.494	1.23	0.10
	2.09 GeV/c	
0.260	8.36	0.28
0.276	6.99	0.25
0.292	6.52	0.23
0.309	5.63	0.21
0.326	4.86	0.19
0.343	4.32	0.18
0.360	3.38	0.16
0.378	2.98	0.14
0.396	2.52	0.13
0.415	2.06	0.12
0.434	1.81	0.11
0.453	1.35	0.09
0.472	1.54	0.10
0.491	1.19	0.09
0.511	0.958	0.080
0.530	0.967	0.081
	2.16 GeV/c	
0.277	7.28	0.16
0.293	6.29	0.15
0.311	5.06	0.13
0.329	4.61	0.12
0.346	3.63	0.11
0.364	3.26	0.10
0.383	2.62	0.09
0.402	2.32	0.08
0.421	1.81	0.07

MORE

Table II. (continued)

$-t$ $(GeV/c)^2$	$d\sigma/dt$ $mb/(GeV/c)^2$	Statistical error $mb/(GeV/c)^2$
0.441	1.58	0.06
0.462	1.30	0.06
0.481	1.10	0.05
0.501	0.948	0.050
0.522	0.805	0.046
0.542	0.658	0.042
0.563	0.606	0.041
	2.23 GeV/c	
0.293	6.11	0.25
0.312	5.23	0.22
0.330	4.41	0.20
0.348	3.67	0.18
0.368	3.07	0.16
0.387	2.75	0.15
0.406	1.99	0.12
0.427	1.80	0.12
0.468	1.27	0.10
0.489	1.00	0.09
0.510	0.845	0.077
0.531	0.637	0.068
0.553	0.574	0.065
0.574	0.495	0.061
0.596	0.346	0.051
	2.31 GeV/c	
0.314	5.29	0.18
0.333	4.14	0.16
0.352	3.53	0.14
0.373	2.99	0.13
0.393	2.33	0.11
0.413	2.01	0.10
0.434	1.64	0.09
0.456	1.41	0.08
0.477	1.20	0.08
0.499	0.939	0.066
0.522	0.723	0.057
0.544	0.632	0.054
0.566	0.542	0.050
0.589	0.456	0.046
0.612	0.339	0.040
0.636	0.369	0.042
	2.41 GeV/c	
0.340	4.42	0.16
0.361	3.53	0.14
0.382	2.74	0.12
0.403	2.54	0.12
0.425	2.00	0.10
0.448	1.56	0.09
0.470	1.17	0.07
0.493	0.914	0.065
0.516	0.801	0.060
0.540	0.637	0.053
0.563	0.533	0.047

MORE

Table II. (continued)

-t $(GeV/c)^2$	$d\sigma/dt$ $mb/(GeV/c)^2$	Statistical error $mb/(GeV/c)^2$	-t $(GeV/c)^2$	$d\sigma/dt$ $mb/(GeV/c)^2$	Statistical error $mb/(GeV/c)^2$
0.587	0.349	0.039	0.444	2.12	0.08
0.611	0.376	0.040	0.468	1.64	0.07
0.637	0.352	0.039	0.494	1.26	0.06
0.661	0.272	0.035	0.520	1.02	0.05
0.685	0.287	0.036	0.546	0.784	0.047
			0.572	0.680	0.043
	2.51 GeV/c		0.598	0.548	0.038
0.367	3.66	0.14	0.626	0.435	0.033
0.390	3.03	0.13	0.653	0.407	0.032
0.413	2.44	0.11	0.681	0.297	0.027
0.435	2.02	0.10	0.708	0.262	0.026
0.459	1.60	0.09	0.736	0.287	0.027
0.482	1.28	0.08	0.764	0.276	0.027
0.506	1.10	0.07	0.792	0.285	0.028
0.531	0.839	0.060			
0.556	0.600	0.049		2.76 GeV/c	
0.581	0.554	0.047	0.439	1.98	0.10
0.607	0.518	0.045	0.466	1.71	0.09
0.632	0.389	0.039	0.493	1.35	0.08
0.659	0.347	0.037	0.520	0.965	0.063
0.685	0.268	0.033	0.547	0.863	0.059
0.711	0.235	0.031	0.576	0.758	0.054
0.738	0.249	0.032	0.605	0.582	0.047
			0.633	0.467	0.041
	2.62 GeV/c		0.663	0.394	0.037
0.395	3.11	0.10	0.692	0.339	0.034
0.420	2.46	0.09			

MORE

Table II. (continued)

-t $(GeV/c)^2$	$d\sigma/dt$ $mb/(GeV/c)^2$	Statistical error $mb/(GeV/c)^2$	-t $(GeV/c)^2$	$d\sigma/dt$ $mb/(GeV/c)^2$	Statistical error $mb/(GeV/c)^2$
0.723	0.339	0.034	0.421	2.00	0.14
0.753	0.291	0.032	0.456	1.38	0.11
0.783	0.340	0.034	0.491	1.02	0.10
0.813	0.241	0.029	0.527	0.734	0.078
0.844	0.219	0.028	0.563	0.675	0.076
0.875	0.196	0.027			
				3.77 GeV/c	
	3.01 GeV/c		0.240	7.60	0.30
0.515	1.20	0.07	0.270	6.45	0.27
0.545	1.00	0.06	0.302	5.52	0.24
0.577	0.755	0.052	0.335	4.13	0.20
0.608	0.611	0.046	0.369	3.26	0.17
0.639	0.496	0.041	0.404	2.47	0.15
0.672	0.435	0.038	0.441	2.01	0.13
0.706	0.364	0.034	0.479	1.17	0.10
0.739	0.334	0.032	0.517	0.757	0.077
0.773	0.283	0.029	0.557	0.536	0.065
0.809	0.266	0.028			
0.842	0.259	0.027		4.02 GeV/c	
0.876	0.275	0.028	0.273	6.54	0.26
			0.306	4.88	0.22
	3.52 GeV/c		0.342	4.20	0.19
0.294	5.92	0.26	0.379	2.89	0.16
0.324	4.66	0.22	0.417	2.25	0.13
0.355	3.20	0.18	0.457	1.82	0.12
0.388	2.60	0.16	0.499	1.02	0.09
			0.541	0.736	0.074

Table II. (continued)

$-t$ $(GeV/c)^2$	$d\sigma/dt$ $mb/(GeV/c)^2$	Statistical error $mb/(GeV/c)^2$
	5.03 GeV/c	
0.274	5.73	0.18
0.316	4.67	0.15
0.363	3.03	0.12
0.410	2.04	0.09
0.461	1.38	0.08
0.514	0.804	0.055
0.570	0.635	0.048
0.627	0.354	0.035
	5.53 GeV/c	
0.281	5.28	0.16
0.328	4.11	0.14
0.379	2.62	0.11
0.434	1.94	0.09
0.492	1.16	0.07
0.553	0.692	0.049
0.614	0.385	0.036

Table III. Parameter b in $d\sigma/dt = Ae^{bt}$, from a fit to the present data for t values $|t| \leq 0.63$ $(GeV/c)^2$

Beam momentum (GeV/c)	Number of data points	χ^2	b $(GeV/c)^{-2}$
1.71	12	6.2	7.91 ± 0.25
1.81	16	16.5	7.30 ± 0.16
1.91	14	7.0	7.76 ± 0.21
2.01	16	23.2	8.02 ± 0.16
2.09	16	21.6	8.55 ± 0.16
2.16	16	17.2	9.08 ± 0.11
2.23	15	4.9	9.24 ± 0.21
2.31	15	6.7	9.06 ± 0.18
2.41	13	11.6	9.63 ± 0.21
2.51	11	7.2	8.81 ± 0.24
2.62	10	4.4	8.73 ± 0.22
2.76	7	5.1	7.53 ± 0.44
3.01	4	0.3	7.40 ± 0.96
3.52	9	5.4	8.64 ± 0.28
3.77	10	28.6	7.77 ± 0.21
4.02	8	12.0	7.70 ± 0.25
5.03	8	12.9	7.93 ± 0.17
5.53	7	13.2	7.50 ± 0.18

FIGURE CAPTIONS

Fig. 1. Plan view of experimental apparatus. The pion beam is incident from the left on a hydrogen target. The scattered pions pass through magnet M1, and counter arrays A and B and are detected in coincidence with recoil protons in the side array P.

Fig. 2. A typical raw data run. The beam momentum is 2.01 GeV/c and the total number of incident pions is 20×10^8. There are 16 event distributions shown in the figure; increasing number means increasing pion scattering angle. The elastic events form a well-defined peak with a background of less than 1%.

Fig. 3. Comparison of our data with data from other experiments near 2.5 GeV/c and 2.1 GeV/c.

Fig. 4. In the lower portion: slope parameter b versus laboratory beam momentum; in the upper portion: total $\pi^- p$ cross section versus laboratory beam momentum. The values of b plotted are taken exclusively from this experiment. The values of σ_T plotted are taken from Carter et al., Ref. 7; and Citron et al., Ref. 10.

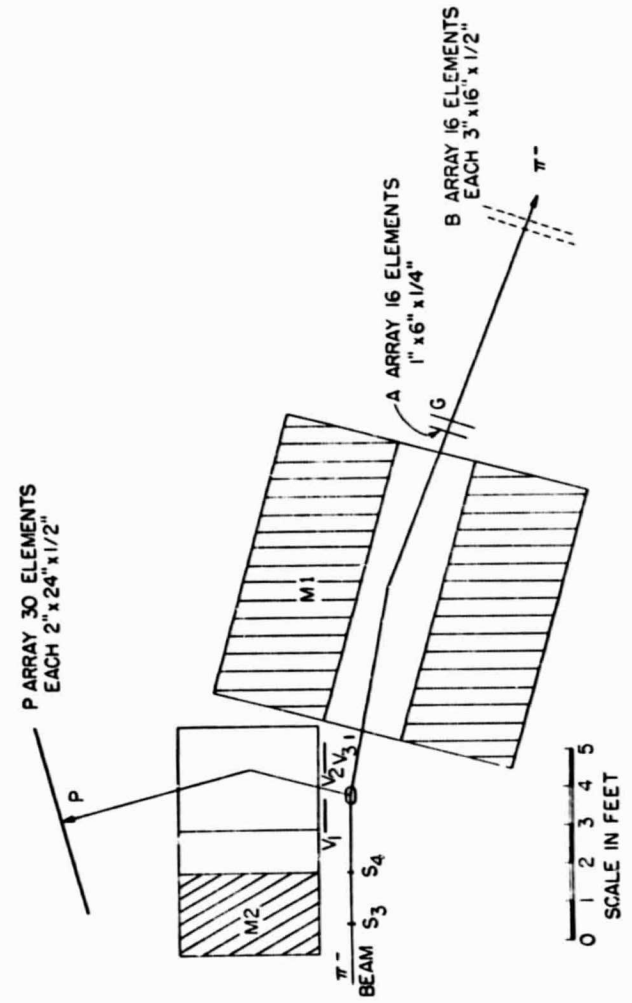

Fig. 1. Plan view of the experimental apparatus. The pion beam is incident from the left on a hydrogen target. The scattered pions pass through magnet M1 and counter arrays A and B and are detected in coincidence with recoil protons in the side array P.

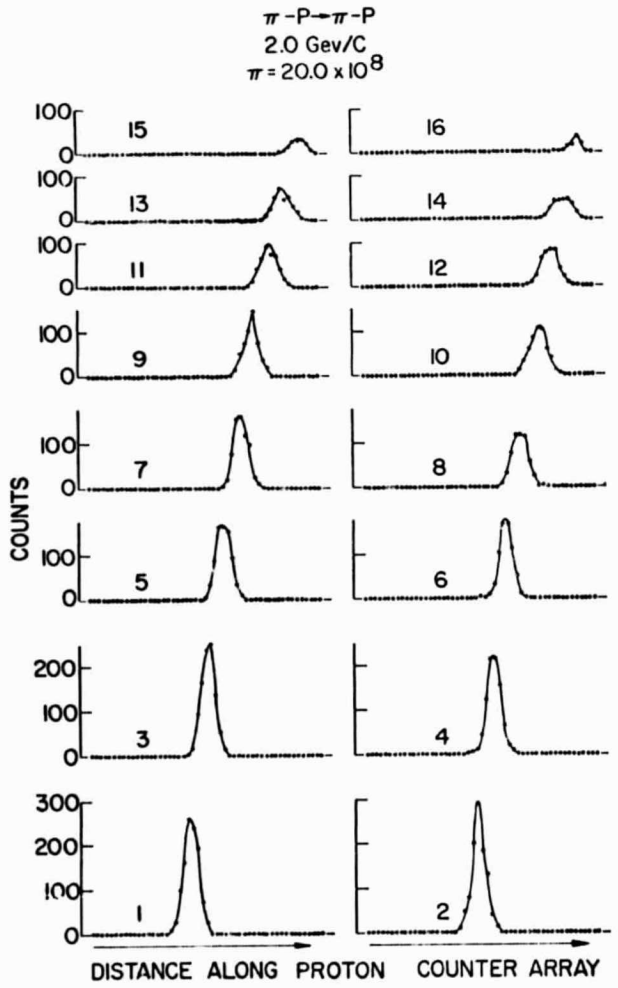

Fig. 2. A typical raw data run. The beam momentum is 2.01 GeV/c and the total number of incident pions is 20 x 10^8. There are 16 event distributions shown in the figure; increasing number means increasing pion scattering angle. The elastic events form a well-defined peak with a background of less than 1%.

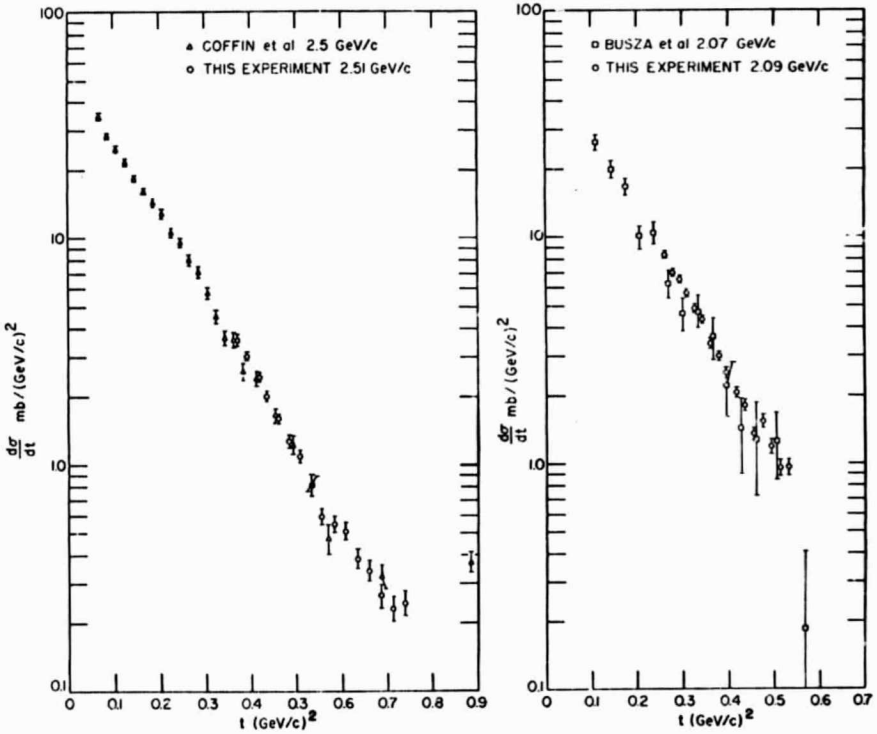

Fig. 3. Comparison of our data with data from other experiments near 2.5 GeV/c and 2.1 GeV/c.

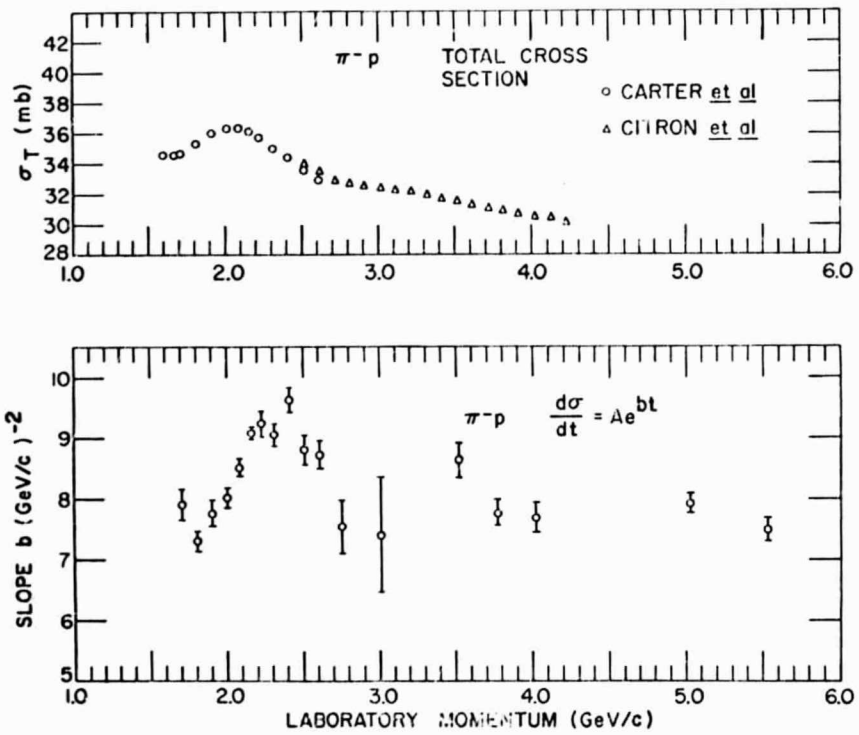

Fig. 4. In the lower portion: slope parameter b versus laboratory beam momentum; in the upper portion: total π^-p cross section versus laboratory beam momentum. The values of b plotted are taken exclusively from this experiment. The values of σ_T plotted are taken from Carter et al., Ref. 7; and Citron et al., Ref. 10.

END

DATE FILMED

2 / 5 / 71